

3D EFFECTS IN RFQ ACCELERATORS

Sergey S. Kurennoy, LANL, Los Alamos, NM, USA

Abstract

RFQ accelerators are usually designed and modeled with standard codes based on electrostatic approximations. Recent examples show that this approach fails to accurately predict the performance for 4-rod RFQs: 3D RF effects near the vane ends can noticeably influence the beam dynamics. The same applies to any RFQ where the quadrupole symmetry is broken, e.g., 4-vane RFQ with windows. We analyzed two 201.25-MHz 4-rod RFQs – one recently commissioned at FNAL and a new design for LANL – using 3D modeling with CST Studio. In both cases the manufacturer CAD RFQ model was imported into CST. The electromagnetic analysis with MicroWave Studio was followed by beam dynamics modeling with Particle Studio. For the LANL RFQ with duty factor up to 15%, a thermal-stress analysis with ANSYS was also performed. The simulation results for FNAL RFQ helped our Fermilab colleagues fix the low output beam energy. The LANL RFQ design was modified after CST simulations indicated insufficient tuning range and incorrect output energy; the modified version satisfies the design requirements.

INTRODUCTION

Radio-frequency quadrupole (RFQ) accelerators are now ubiquitous in front ends of modern ion linacs. Usual RFQ design codes, e.g., Parmteq [1], rely on electrostatic field approximations that are well justified for classical 4-vane RFQs with perfect quadrupole symmetry. On the other hand, many modern RFQs contain elements that break this symmetry. RFQ vane modulations introduce perturbations that create a longitudinal accelerating field, which is the basic idea of the RFQ. The vane-modulation effects are accounted in analytical field representation in the codes or can be calculated by solving an electrostatic problem. However, additional RF field effects can be introduced by asymmetric elements like vane windows in split-coax designs or stem supports in 4-rod RFQs. Such effects are more complicated and can't be easily taken into account in electrostatic calculations, even in 3D, but can influence beam dynamics in some cases. We discuss 3D RF effects in two 4-rod RFQs that we have recently analyzed in details [2, 3] with CST Studio [4].

RFQ MODELS

Having an accurate model of the RFQ cavity is important for its EM analysis. For both RFQs considered, a CAD model from the manufacturer Kress GmbH was imported into CST. The model was further simplified by removing details unessential for EM calculations. The RFQ cavity outer walls were also removed, leaving only the resonator vacuum volume in the CST model. The outer boundaries are assumed perfect-conducting for EM

simulations. The resulting model for the new LANL RFQ is shown in Fig. 1. The RFQ vacuum vessel, in light-blue, is 175-cm long and contains 24 stems. The tuners between the adjacent stems (Fig. 1, bottom) are at different heights. They are adjusted in the CST model to make the inter-vane voltage flat, see Ref. [3].

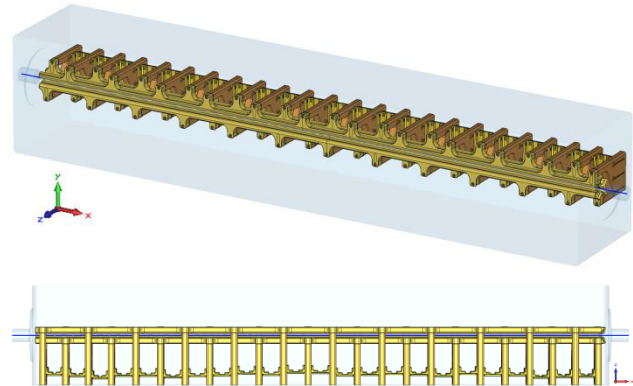


Figure 1: CST RFQ model (top) and its side view.

ELECTROMAGNETIC ANALYSIS

We studied the RFQ models using the CST MicroWave Studio (MWS). The mode frequencies and RF fields were calculated by the AKS eigensolver that provides more accurate surface approximations. In the latest CST version of 2014 the CAD import has been improved, which may allow using its more efficient tetrahedral eigensolver. The calculated RF fields have some interesting features. The first one is the presence of the longitudinal electric field in the end gaps that separate the vane ends from RFQ cavity walls. These end-gap bumps are illustrated in Fig. 2 for the FNAL 4-rod RFQ, cf. [5].

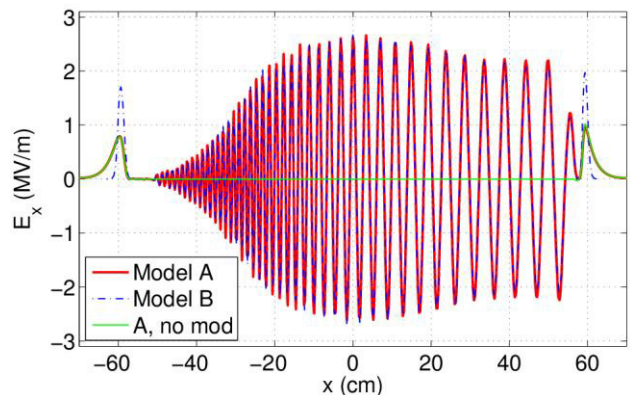


Figure 2: On-axis longitudinal field in FNAL RFQ.

Two models of the FNAL RFQ were studied [2]: model A with wide beam pipes attached to the RFQ cavity and model B with narrow beam pipes. The RFQ accelerating field (the oscillating part of the curves in Fig. 2) is produced by the vane modulation. The longitudinal field

in Fig. 2, however, also has two peaks, near the RFQ entrance and exit. The RFQ cavity extends from $x = -60$ cm to $x = 60$ cm, so the RF fields spread into the beam pipes. The end-gap longitudinal field exists because the quadrupole symmetry is broken near the ends; it would vanish in a perfectly symmetric structure. The end-gap bumps depend on the diameter of beam pipes attached to the RFQ, cf. Fig. 2, while the accelerating fields coincide in the two models. In model B, the narrow beam pipes trap the fields in the gaps, so the peaks are higher and shorter. If we remove the vane modulation in model A, the accelerating field disappears as expected, but the end-gap bumps remain the same as with modulation (the green curve in Fig. 2)

The exit-end bump can change the output beam energy depending on the beam transit-time factor in the exit gap. It was the reason for the low output energy in the FNAL RFQ in its original configuration (B). Opening the exit beam pipe by removing an end-wall plug (change from B to A) restored the design energy [5].

Important to note that 3D electrostatic computations of 4-vane quadrupole structure do not exhibit bumps since the static field remains quadrupole-symmetric, cf. Fig. 3. However, even in 4-vane RFQs with cuts that distort the symmetry, e.g., the split-coaxial structure [6], the end-gap peaks are present, though in the particular case [6] they do not influence beam dynamics as drastically as here.

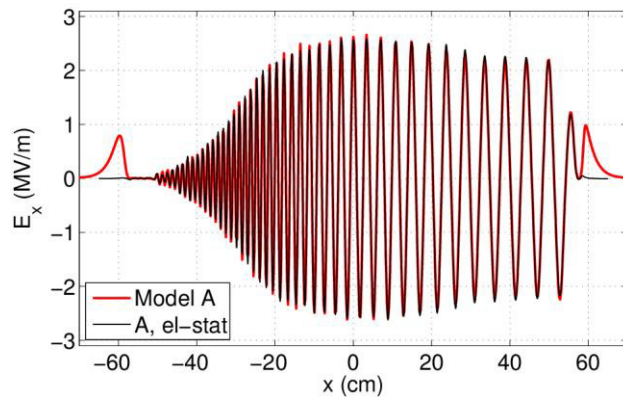


Figure 3: On-axis longitudinal field: RF vs. electrostatic.

Another feature typical for 4-rod RFQs is a small transverse horizontal (parallel to the RFQ ground plane) field component on its geometrical axis. It is illustrated in Fig. 4 that plots LANL RFQ on-axis field components: longitudinal E_l , horizontal E_h , and vertical E_v (along the stems) versus the longitudinal coordinate s . Here $s = -x$ because in the RFQ model of Fig. 1 the beam travels from right to left. This effect is due to the fact that the transverse electric fields between two upper vanes are stronger than between two lower ones. It results in the displacement of the center of the transverse quadrupole field down, to the ground plane, from the RFQ axis by 0.45 mm, to be compared to the 4-mm vane aperture. The effect is known in higher-frequency 4-rod RFQs [7]. We found no noticeable influence of this feature on beam dynamics in the two 4-rod RFQs that we studied [2, 3].

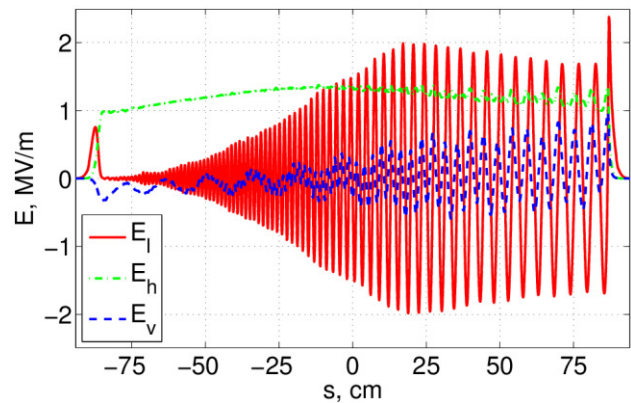


Figure 4: On-axis field components in LANL RFQ.

The end-gap bumps of the longitudinal field can also be seen in Fig. 4; their effect was taken into account in beam dynamics simulations. The initial design of the LANL RFQ was modified based on our simulation results to adjust the frequency tuning range and the final energy [3].

BEAM DYNAMICS

Multi-particle beam dynamics modeling based on the MWS calculated RF fields can be performed with either the CST Particle Studio (PS) particle-in-cell (PIC) solver or other codes. We cross-checked our PS results for the new LANL RFQ with two well-known dynamics codes, Parmela [1] and Beampath [8], and the results agree well. The important part was to use accurately calculated by MWS RF fields that include 3D effects discussed above.

Matched CW beams of 10K macro-particles, one RF period long, were generated for several different currents using matched-beam Twiss parameters at the RFQ vane entrance and tracing particles back to the beam-pipe entrance. These distributions were repeatedly injected into the PS model during many RF periods. PS simulations of RFQs can be significantly sped up if the model simulation volume is cut transversely to a narrow region around the aperture for particle runs. This allows us to run beams up to 500 RF periods long on a PC; see details in [3, 9, 10]. As an illustration, Fig. 5 shows a snapshot of the LANL RFQ PS model running a very high current of 60 mA with 500x10K macro-particles. The particles propagate from right to left. The number of particles at this moment is about 788K; most of them are densely packed in bunches (colored blobs). The particle energy is indicated by color; cf. the energy scale on the right, from 17.5 to 805 keV. Trailing low-energy particles are not captured in bunches.

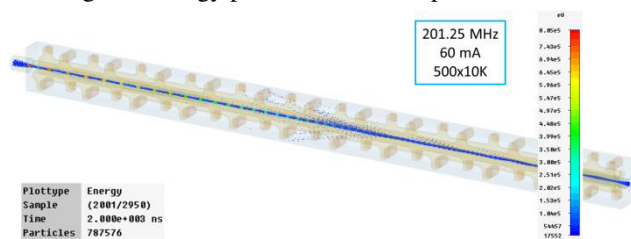


Figure 5: Particles in the LANL RFQ model with 60 mA.

PS simulations results for the average energy W , transverse normalized rms emittance ϵ_t , longitudinal emittance ϵ_l , and current transmission are summarized in Table 1. The initial distribution had a normalized rms transverse emittance $0.2 \pi \text{ mm}\cdot\text{mrad}$ in both planes.

Table 1: Results for Different Currents in LANL RFQ

I , mA	W , keV	ϵ_t , π mm·mrad	ϵ_l , keV·deg	Trans- mission
0	756	0.25	128	0.99
12	756	0.26	85	0.97
24	754	0.25	79	0.94
35	753	0.27	87	0.88

THERMAL ANALYSIS

Calculating 3D RF fields is essential to find accurately the current distribution and thermal load, especially for high-duty RFQs. The LANL RFQ is designed to operate at noticeable duty factors, up to 15%, so the structure thermal and stress analysis has been performed [3]. The heat flux, calculated in post-processing the MWS-computed RF fields, was used for thermal-stress analysis with ANSYS [11]. The dissipated power is 77 kW at 100% duty for ideal copper surfaces. Cooling is provided by water running through cooling channels in stems and vanes. The temperature distribution in a structure slice near the RFQ exit is shown in Fig. 6 for the duty factor of 18% (1.2-15%, to take into account realistic surface conductivity). The temperature range is less than 40° C even in this extreme case. The maximal structure deformations were also found acceptable [3].

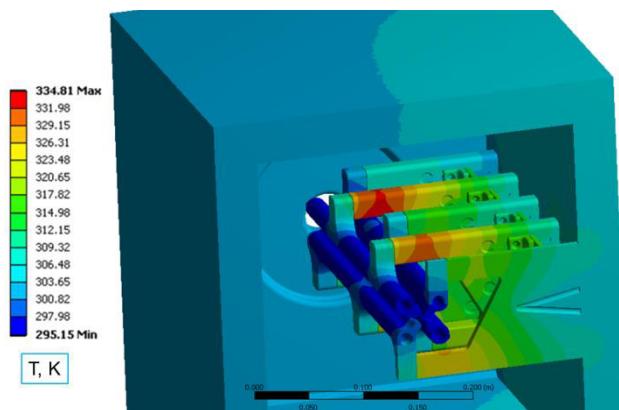


Figure 6: Temperature distribution from ANSYS [3].

A very good recent example of the combined EM and thermal-structural analysis was presented in [12] for an upgrade of the SARAF continuous-wave RFQ to a new four-vane structure. Results of 3D RF calculations were applied to optimize the structure cooling and ensure reliable performance of the RFQ.

CONCLUSION

Detailed 3D modeling of RFQs is now possible with CST Studio. It includes importing or building a 3D CAD model followed by its EM analysis and multi-particle beam dynamics PIC simulations plus thermal and stress engineering analysis for high-duty RFQs. We successfully used this approach for two 4-rod RFQs with CST Studio running on a PC. Our results demonstrate that 3D RF effects, which were not found by standard design and analysis, are very important in these two cases because they significantly influence the RFQ performance.

Other groups have used different tools, see Refs. [6, 12, 13], for building RFQ models, their EM and thermal analysis, and beam dynamics studies. Independent of a particular choice of tools, this modern 3D approach for RFQ design and analysis predicts the RFQ performance more reliably compared to the standard RFQ design codes. There are many reasons to expect that it will be used more widely in future RFQ projects.

ACKNOWLEDGMENT

The author would like to thank R. Garnett, Y. Batygin, L. Rybarcyk, J. O'Hara, E. Olivas, and T. Wangler for support and help at various stages of this work, useful information, and stimulating discussions. Help from and discussions with our FNAL and German colleagues are also acknowledged.

REFERENCES

- [1] Los Alamos Accelerator Code Group, laacg.lanl.gov
- [2] S.S. Kurennoy et al., "EM and Multi-particle Beam Dynamics Modeling of 4-Rod RFQs," IPAC2013, Shanghai, China, p. 3978 (2013); www.JACoW.org
- [3] S.S. Kurennoy et al., "Design Analysis of the New LANL 4-Rod RFQ," PAC2013, Pasadena, CA USA, p. 333 (2013); www.JACoW.org
- [4] CST Studio Suite, www.cst.com
- [5] J.S. Schmidt et al., Phys. Rev. ST Accel. Beams 17, 030102 (2014).
- [6] B. Mustapha et al., Phys. Rev. ST Accel. Beams 16, 120101 (2013).
- [7] B. Kubek et al., PAC11, New York, USA, p. 1888 (2011); www.JACoW.org
- [8] Y.K. Batygin, Nucl. Instr. Meth. A539, 455 (2005).
- [9] S.S. Kurennoy, "EM and Beam-Dynamics Modeling of the New LANL RFQ with CST Studio," report LA-UR-13-28693, Los Alamos (2013).
- [10] S.S. Kurennoy et al., "Realistic Modeling of 4-Rod RFQs with CST Studio," IPAC2014, Dresden, Germany, p. 3119 (2014); www.JACoW.org
- [11] ANSYS Inc., www.ansys.com
- [12] S.V. Kutsaev et al., Phys. Rev. ST Accel. Beams 17, 072001 (2014).
- [13] S. Jolly et al., Nucl. Instr. Meth. A735, 240 (2014).